

# Molecular Cloning and Functional Expression of Mouse Connexin40, a Second Gap Junction Gene Preferentially Expressed in Lung

Hanjo Hennemann, Tom Suchyna,\* Hella Lichtenberg-Fraté, Stefan Jungbluth, Edgar Dahl, Jürgen Schwarz, Bruce J. Nicholson,\* and Klaus Willecke

Institut für Genetik, Abt. Molekulargenetik, Universität Bonn, 5300 Bonn 1, Germany; and \*Department of Biological Sciences, State University of New York at Buffalo, Buffalo, New York 14260

**Abstract.** From a mouse genomic library, a clone has been isolated that codes for a connexin-homologous sequence of 358 amino acids. Because of its theoretical molecular mass of 40.418 kD it is named connexin40 (Cx40). Based on both protein and nucleotide sequence, mouse Cx40 is more closely related to mouse Cx43 ( $\alpha$  subgroup of connexins) than to mouse Cx32 ( $\beta$  subgroup). The highest overall homology detected, however, was to chick Cx42 (67% amino acid and 86% nucleotide identity), raising the possibility that Cx40 may be the mouse analogue. The coding region of Cx40 is uninterrupted by introns and is detected as a single copy gene in the mouse genome. High stringency hybridization of Northern blots with the coding sequence of Cx40 identified a single transcript of 3.5 kb that is at least 16-fold more abundant in lung—similar to mouse Cx37—than in other adult tissues (kidney, heart, and skin). In embryonic kidney, skin, and liver the level of the Cx40 transcript is two- to

fourfold higher than in the corresponding adult tissues. Microinjection of Cx40 cRNA into *Xenopus* oocytes induced functional cell-to-cell channels between pairs. These channels show a symmetrical and markedly cooperative closure in response to transjunctional voltage (Boltzmann parameters of  $V_o = \pm 35$  mV;  $A = 0.32$ ) which is also fast relative to other connexin channels recorded similarly ( $\tau = 580$  ms at  $V_j$  of  $\pm 50$  mV). Although Cx40-expressing oocytes did not couple efficiently with oocytes expressing endogenous connexins, they did couple well to Cx37-expressing oocytes. The heterotypic channels which formed had voltage-gating properties modified from those of the original homotypic forms. Transfection of mouse Cx40 DNA, under control of the SV-40 early promoter, into coupling-deficient human HeLa or SK-Hep-1 cells resulted in expression of the expected transcript and restoration of fluorescent dye transfer in transfected clones.

**C**ONNEXINS are structural proteins that form the subunits of the cell-to-cell channels of gap junctions. So far five rat connexins have been designated according to their molecular mass deduced from analyses of cDNA or genomic clones: connexin32 (Cx32) (Paul, 1986; Kumar and Gilula, 1986; Heynkes et al., 1986), Cx43 (Beyer et al., 1987), Cx46 (Beyer et al., 1988), Cx26 (Zhang and Nicholson, 1989), and Cx31 (Hoh et al., 1991). Recently we have characterized mouse Cx37 (Willecke et al., 1991b) and have presented evidence that at least four more connexins exist in the mouse genome (i.e., Cx30.3, Cx31.1, Cx40, and Cx45) Willecke et al., 1991a, in addition to the analogues of those previously described in rat (these show amino acid identities  $> 98\%$  and nucleotide identities  $> 92\%$  between the two species [Willecke et al., 1990a]). Based on peptide-specific antibody labeling and limited proteolysis of isolated gap junctions containing Cx32, Cx26, or Cx43, it has been deduced that the polypeptide chain of connexins spans the plasma membrane four times with the NH<sub>2</sub>- and COOH-terminal regions plus a central "loop" facing the cytoplasm (Milks et al., 1988; Hertzberg et al., 1988; Beyer

et al., 1989; Yancey et al., 1989). Connexins are highly homologous in the transmembrane regions and the two extracellular loops, but have major differences in both the length and sequences of the cytoplasmic loop and COOH-terminal domain.

The finding that the connexin family consists of at least 10 different members in mouse and presumably all mammals suggests that each may be functionally specialized (Willecke et al., 1991a). Consistent with this is the observation that different connexins appear to form channels of different conductance (compare channels of 160 pS and 50–60 pS in myocytes [Veenstra and DeHaan, 1986; Burt and Spray, 1988]; 120 pS in hepatocytes [Spray et al., 1986]; and 120–150 pS in Cx32 transfected in SK-Hep-1 cells [Eghbali et al., 1990]). This suggests that each connexin may have its own characteristic permeability. Furthermore, posttranslational phosphorylation, which has been associated with modulation of gap junction function, is different among connexins. For example, Cx32 is phosphorylated by cAMP-dependent kinase (Saez et al., 1986), but Cx26 is not (Traub et al., 1989). Cx43 is most readily phosphorylated by protein ki-

nase C (Kadle, R., and B. J. Nicholson, unpublished observations) and src tyrosine kinase (Swenson et al., 1990). Evidence of functionally significant differences is provided by the expression of different connexin genes in coordination with the cell differentiation programs in each tissue. Further complexity to this pattern is contributed by the overlapping expression of several connexins. For example, Cx32 and Cx26 are both expressed in the same gap junction plaques of hepatocytes (Nicholson et al., 1987) and are capable of forming heterotypic (different connexins in apposed cells) if not heteromeric (different connexins in the same hemichannel) junctional channels (Barrio et al., 1991).

In this report we describe a new mouse connexin, Cx40, whose sequence appears to be related to chick Cx42, although the overall amino acid identity is only 67%. Mouse Cx40 mRNA shows a similar pattern of tissue expression to mouse Cx37. While Cx40 forms intercellular channels with unique properties when expressed in *Xenopus* oocytes, these channels can also interact with those of Cx37 to form heterotypic channels with somewhat modified properties.

## Materials and Methods

### Cells and Culture Conditions

Human cervix carcinoma HeLa (ATCC CCC2) cells and human adenocarcinoma SK-Hep-1 cells (ATCC HTB 52) were cultured in DME supplemented with 10% FCS, 100 U/ml penicillin, and 100 µg/ml streptomycin (standard medium) at 37°C in a moist atmosphere of 10% CO<sub>2</sub>.

### DNA Libraries and Isolation of Genomic Mouse Cx40 DNA

The mouse genomic library used was the same as described by Willecke et al. (1991b). The procedure for isolation of purified phage clones from a genomic EMBL3 mouse library was described in Willecke et al. (1991b). To determine which connexin genes were represented in these phages 2 µl of lysate from each purified plaque was spotted onto a lawn of *Escherichia coli* LE392 on a BBL agarose (Seakem; FMC Corp., Rockland, ME) plate and incubated overnight at 37°C. The next day a Hybond-N, filter (Amersham International, Amersham, Great Britain) was drawn and subjected to hybridization with various connexin cDNAs and gene probes under stringent conditions (50% formamide, 42°C, 5 × SSC). These probes represented part of the coding regions of mouse Cx30.3 and Cx31.1 (Willecke et al., 1991a), rat Cx32, Cx43, Cx46, and mouse Cx37. No recombinant phage clones harboring Cx43 gene sequences could be found. Several phage clones were identified that did not hybridize to any of these connexin gene probes. One of these latter phages (clone 6c) was isolated using standard protocols (Sambrook et al., 1989). This DNA was digested with different restriction enzymes alone, or in combination with Sall, which cuts off the phage arms. From Southern blot hybridization data on the digested phage DNA, it was concluded that a 7-kb XbaI fragment contained the sequence homologous to the rat Cx26 cDNA probe. This fragment was subcloned into the plasmid vector pUC19. Insert DNA of this clone was purified from a low melting agarose gel and partially digested with the restriction enzyme PvuII. The resulting fragments were then subcloned in pUC19. A 2.1-kb PvuII/XbaI fragment, hybridizing to the Cx26 probe, was sequenced by a modification of the chain termination method (Tabor and Richardson, 1987) using either vector-derived oligonucleotide primers or appropriate primers derived from previous sequencing results. The amino acid sequence deduced from the longest open reading frame (i.e., Cx40) was aligned with different connexin sequences with the Microgenie sequence analysis program (Beckman Instrs., Inc., Fullerton, CA).

### Isolation of Genomic Mouse Cx43 DNA

The genomic mouse library was screened with a Cx43 cDNA probe from rat (Beyer et al., 1987). EMBL3 phages (600,000) were transferred to four

square filters (20 cm × 20 cm, Hybond-N; Amersham International) and hybridized to the Cx43 cDNA probe labeled by random priming (8.5 × 10<sup>5</sup> cpm/ml; sp act: 6.8 × 10<sup>8</sup> cpm/µg DNA) according to a standard protocol of plaque hybridization (Sambrook et al., 1989). Hybridization was performed under lowered stringency at 38°C, 40% formamide, and 5 × SSC. Only the final rescreening was done using stringent hybridization conditions (50% formamide, 5 × SSC, 42°C) to select for phage clones containing sequences of the mouse Cx43 gene. Six phage clones were purified and DNA was characterized as described above for the Cx40 DNA. One phage clone contained a 1.3-kb EcoRI-SalI fragment while another clone contained an 8-kb EcoRI fragment hybridizing to the rat Cx43 cDNA probe. These fragments were subcloned in the vector pBluescript SK+ (Stratagene Inc., La Jolla, CA) and sequenced as described above.

### Southern and Northern Blot Analysis

Total RNA from tissues or cultured cells was isolated using the guanidinium isothiocyanate/cesium chloride method of Chirgwin et al. (1979). Equal amounts (20 µg) of total RNA from each tissue assayed were used for electrophoresis. RNA from tissue samples and 3.5 µg of the RNA ladder (Gibco Laboratories, Grand Island, NY) were electrophoresed in 1.2% agarose in the presence of 2.2 M formamide (Sambrook et al., 1989). After ethidium bromide staining the RNA was blotted onto Hybond-N membranes. Afterwards the gel was checked for quantitative transfer by UV-transillumination. High stringency hybridizations of the mouse tissue Northern blot were done as described in Willecke et al. (1991b) using as a probe either a labeled genomic Cx40 fragment (PstI-PvuII) of the coding region or the labeled Cx37 cDNA (Willecke et al., 1991b). For consecutive hybridizations, the previous gene probe was removed by pouring a boiling solution of Tris-HCl (1 mM, pH 7.5) and 0.1% (wt/vol) SDS onto the filters and cooling down to room temperature. Filters were autoradiographed to ensure that removal of the probe had been successful.

To compare the amounts of Cx40 and Cx37 transcripts, dot blots of the corresponding unlabeled DNA probe were prepared. Successive 10-fold dilutions (1 ng–0.1 pg) of either the Cx40 fragment containing the coding region, ranging from position –24 to 81 bp past the stop codon, or the 1.5-kb Cx37 cDNA were spotted as dots onto Hybond-N membranes in the presence of 15 × SSC. The dot blot and a Northern blot with total mouse lung RNA were simultaneously hybridized to the Cx40 and Cx37 probe under the conditions described above. RNA and dot blot signals on autoradiographs were quantified by densitometric evaluation using an Ultrascan laser densitometer (Pharmacia LKB Biotechnology Inc., Sweden). From the Northern/dot blot double-hybridization experiment, the relative amounts of Cx40 and Cx37 transcript in lung were estimated and used to standardize the results of both Northern blot hybridizations. The amounts of poly(A)<sup>+</sup> RNA on Northern blots were estimated by hybridization to the 1.58-kb EcoRI-SalI fragment of mouse cytochrome c oxidase cDNA (clone pAG82; Herget et al., 1989).

DNA from the liver of BALB/c mice was prepared according to a standard procedure (Sambrook et al., 1989). Restriction endonuclease-digested genomic mouse DNA (8 µg) was electrophoresed in 0.7% agarose and blotted by alkaline transfer onto Hybond-N membrane following the manufacturer's procedure (Amersham International). The Southern blot hybridization with Cx40 was carried out under the same conditions as described for Northern blot hybridizations except that 50% formamide was used for hybridization.

### Oocyte Expression and Physiological Analysis

Stage VI oocytes from *Xenopus laevis* toads were defolliculated, injected, stripped of their vitelline membranes, and paired as described in Willecke et al. (1991b). Each oocyte was injected with 40 nl of 0.05 mg/ml cRNA for Cx40, either alone, or in combination with 0.2 mg/ml of antisense oligonucleotide to *Xenopus* Cx38 (nucleotides 327–358). The latter served to eliminate any contribution from endogenous coupling (see Barrio et al., 1991; Willecke et al., 1991b). Five prime capped cRNA was synthesized in vitro by SP6 RNA polymerase using an EcoRI-linearized SP64 plasmid DNA containing a 1.1-kb fragment with the complete Cx40 coding sequence inserted between the 5' and 3' nontranslated regions of β globin cDNA from *Xenopus* (SP64T vector; see Krieg and Melton, 1984). The 1.1-kb fragment had been derived from the 2.1-kb PvuII fragment by truncation of the 5' end using exonuclease III. This left only 24 nucleotides upstream of the initiator ATG. No other ATGs were present in the remaining flanking sequence. 48 h after injection oocytes were paired, and junctional conductance was recorded 24–36 h later by dual cell voltage clamp as described in Willecke et al. (1991b). All oocytes used had resting potentials between –36 and –58

mV and were voltage clamped between -40 and -50 mV. Resting potentials of paired oocytes never varied by more than 5 mV. Values for initial (I) and steady-state (ss) conductance were obtained by fitting each current decay to an exponential and extrapolating to zero or infinity, respectively.  $G_j$  (i) was normalized to its value at  $\pm 10$  mV and, unless otherwise noted,  $G_j$  (ss) was normalized to the value of  $G_j$  (i) at the same voltage.

### Transfections of Human Cells and Analysis of Cx40 Transfectants

The 1.2-kb BamHI-KpnI fragment of the mouse Cx40 gene, derived from the pBluescript SK/Cx40 construct, containing the 1.1-kb coding region in the HincII site, was ligated to DNA of the vector pBEHpacl8 (Horst et al., 1991) cut with KpnI and BamHI. This vector contains the SV-40 early promoter as well as polyadenylation signals and a gene conferring resistance to puromycin. HeLa and SK-Hep-1 cells ( $10^6$  each) were transfected with 20  $\mu$ g of the recombinant plasmid pBEHpacl8/Cx40 using the calcium phosphate transfection protocol of Chen and Okayama (1987). 64 h after transfection the standard medium was replaced by fresh standard medium containing 1  $\mu$ g puromycin/ml (for HeLa cells) or 2  $\mu$ g puromycin/ml (for SK-Hep-1 cells). Individual clones were picked after 3 wk and grown in selective medium for subsequent analyses.

Northern blot hybridizations were carried out as described above. Dye transfer was measured in subconfluent cultured cells after iontophoretic injection of Lucifer yellow (4% wt/vol in 1 M LiCl) as previously published (Traub et al., 1989). The injected cells were monitored 1 min after injection by inspection in fluorescent light and in phase contrast using an AxioPhot microscope (Carl Zeiss, Inc., Oberkochen, Germany). Photographs were taken on Ilford HP5 Plus film. Communication frequencies indicate the proportion of cells showing dye transfer to one or more neighboring cells of the first order.

## Results

### Genomic Sequences of Mouse Cx40 and Mouse Cx43

By screening a mouse genomic library of EMBL3 lambda phages with rat Cx26 cDNA under low stringency of hybridization (38°C, 50% formamide, and 5 $\times$  SSC), a recombinant phage was isolated which contained, within a 16-kb DNA insert, a 7-kb XbaI fragment that hybridized to the probe used. A 2.1-kb fragment, assumed to contain the hybridizing sequence, was isolated after partial digestion by PvuII and sequenced (see Materials and Methods). The longest open reading frame coded for an amino acid sequence of 40.418 kD (Fig. 1) that is similar to other connexins of the Cx43 ( $\alpha$ ) subfamily (see below). Thus we designated this new connexin mouse Cx40 according to the suggested nomenclature (Beyer et al., 1987, 1988). This reading frame included an initiation and termination codon and was uninterrupted by introns, a common feature of all connexin genes characterized to date. At position -34 upstream of the start codon a possible splice acceptor site is located that is preceded by a putative lariat sequence at positions -69 to -63. The coding sequences of the rat Cx32 and the human Cx43 genes are likely to be also preceded by an intron that ends 16 bp upstream of the start of translation (Miller et al., 1988; Fishman et al., 1990). A putative splice acceptor site has also been found 18 bp upstream of the mouse Cx37 coding sequence (Willecke et al., 1991b), although functional verification of these sites in both Cx37 and Cx40 will require either the corresponding cDNA sequence or S1-nuclease protection assays.

Southern blot hybridization with the Cx40 coding region (i.e., the 2.2-kb PvuII-XbaI fragment) to mouse genomic DNA digested with different restriction endonucleases (Fig. 2) indicated that a single copy of the Cx40 gene exists in the

```

-110 -100 -90 -80 -70
GATCAGTGGCCAGAGCATGATGGGACCTTCTAAACCTCTGAAGCATCCCTCCTGAAAC
-50 -40 -30 -20 -10
GTCCTGTGTTTC TGCTCTGTTGCGAG AAGGCTCGGCTCGGTCTCCTACTCTGGCAAG

1 10 20 30 40 50 60
ATGGGTGACTGGAGCTTCTGGGGAGTTCCTGGAGGAGTCCACAAGCACTCCACAGTC
MetGlyAspTrpSerPheLeuGlyGluPheLeuGluGluValHisLysHisSerThrVal
70 80 90 100 110 120
ATCGGCAAGGCTCGGCTCAGTCTGTTTTCATTTCCGGATGCTGGTCTGGGCACCGCT
IleGlyLysValTrpLeuThrValLeuPheIlePheArgMetLeuValLeuGlyThrAla
130 140 150 160 170 180
GCTGAGTCTCTGGGAGATGAGCAGGCCGACTTCCGGTGGCAGTACCATTCCAGCTCGT
AlaGlySerSerTrpGlyAspGluGlnAlaAspPheArgCysAspThrIleGlnProGly
190 200 210 220 230 240
TGCCAAAATGTCTGTATGACCAAGCCTTCCCATCTCCACATTCGTTATGGGTACTG
CysGlnAsnValCysTyrAspGlnAlaPheProIleSerHisIleArgTyrTrpValLeu
250 260 270 280 290 300
CAGATCATCTTTGTGTCCAGCCTTCTAGTGTACATGGCCATGCCATGCCACATGTC
GlnIleIlePheValSerThrProSerLeuValTyrMetGlyHisAlaMetHisThrVal
310 320 330 340 350 360
CGCATCGGAAAAGCAGAAATTCGGGATGCTGAGAAAGTAAAGAGGCCACCCGACT
ArgMetGlnGluLysGlnLysLeuArgAspAlaGluLysAlaLysGluAlaHisArgThr
370 380 390 400 410 420
GGTGCCTATGAGTACCCAGTAGCCGAAAAGGCCGAGCTCTCTGCTGGAAAGAAGTAGAT
GlyAlaTyrGluTyrProValAlaGluLysAlaGluLeuSerCysTrpLysGluValAsp
430 440 450 460 470 480
GGGAAGATTGCTCCAGGGCCACTTACTCAACACCTATGTCTGACCATTCTGATCCGC
GlyLysIleValLeuGlnGlyThrLeuLeuAsnThrTyrValCysThrIleLeuIleArg
490 500 510 520 530 540
ACCACATGGAGGTGGCCTTCATCGTAGCCAGTACTCTCTATGGATCTTCCCTGGAT
ThrThrMetGluValAlaPheIleValGlyGlnTyrLeuLeuTyrGlyIlePheLeuAsp
550 560 570 580 590 600
ACCTGCATGTCTGCCGAGGAGTCCCTGTCCCAACCCAGTCACTGTTATGTTTCGAGG
ThrLeuHisValCysArgArgSerProCysProHisProValAsnCysTyrValSerArg
610 620 630 640 650 660
CCCACGGAGAAGAATGCTTTCATTGCTTTATGATGGCTGGGCTGGACTGTCTCTGTTT
ProThrGlyLysAsnValPheIleValPheMetAlaValAlaGlyLeuSerLeuPhe
670 680 690 700 710 720
CTCAGCTGGCTGAACCTACCCACCTGGGCTGGAAGAAGTCCGACAGCGCTTGGCAAG
LeuSerLeuAlaGluLeuTyrHisLeuGlyTrpLysLysIleArgGlnArgPheGlyLys
730 740 750 760 770 780
TCACGGCAGGGTGGACAAGCACCAGCTGCTGCCCTCCCAACCCAGCTCGTCCAGAGC
SerArgGlnGlyValAspLysHisGlnLeuProGlyProProThrSerLeuValGlnSer
790 800 810 820 830 840
CTCACTCTCCCTCAATCAGTCCCTAAAGAAGCAGCTCCGGAGAGAAATTCCTTC
LeuThrProProProAspPheAsnGlnCysLeuLysAsnSerSerGlyGluLysPhePhe
850 860 870 880 890 900
AGCGACTTCAGTAATAACATGGGCTCCCGGAAGAATCCAGACGCTCTGGCCACTGGGGAA
SerAspPheSerAsnAsnMetGlySerArgLysAsnProAspAlaLeuAlaThrGlyGlu
910 920 930 940 950 960
GTGCCAAACCCAGGAGCAGATTCCAGGGGAGGCTTCCATGCATGCACTATAGCCAGAAG
ValProAsnGlnGluGlnIleProGlyGluGlyPheIleHisMetHisTyrSerGlnLys
970 980 990 1000 1010 1020
CCAGAGTAGCCAGTGGAGCCTCTGCGGCCACCGCTTCCCTCAGGCTACCATAGTGAC
ProGluTyrAlaSerGlyAlaSerAlaGlyHisArgLeuProGlnGlyTyrHisSerAsp
1030 1040 1050 1060 1070 1080
AAACGGCGCTTAGTAAGCCAGCAGCAAAGCAAGTTCAGATGACCTGTCAGTGTGATCC
LysArgArgLeuSerLysAlaSerSerLysAlaArgSerAspLeuSerVal
1090
TCCTTTAGGGAGGCCAG

```

**Figure 1.** Genomic nucleotide and deduced amino acid sequence of mouse Cx40. At the 5' end a potential splice acceptor site (boxed) and a possible lariat formation sequence (at -69 to -63) indicate a potential intron at this position similar to other connexin genomic sequences published (Miler et al., 1988; Fishman et al., 1990). The predicted four transmembrane regions are underlined. The sequence data are available from EMBL/GenBank/DBJ under accession No. X61675.

mouse genome. Under these conditions, single DNA fragments of ~5.4 and 7.2 kb were obtained after treatment with BamHI and XbaI, respectively. The two bands of ~1.4 and 2.9 kb obtained after digestion with HincII are due to a

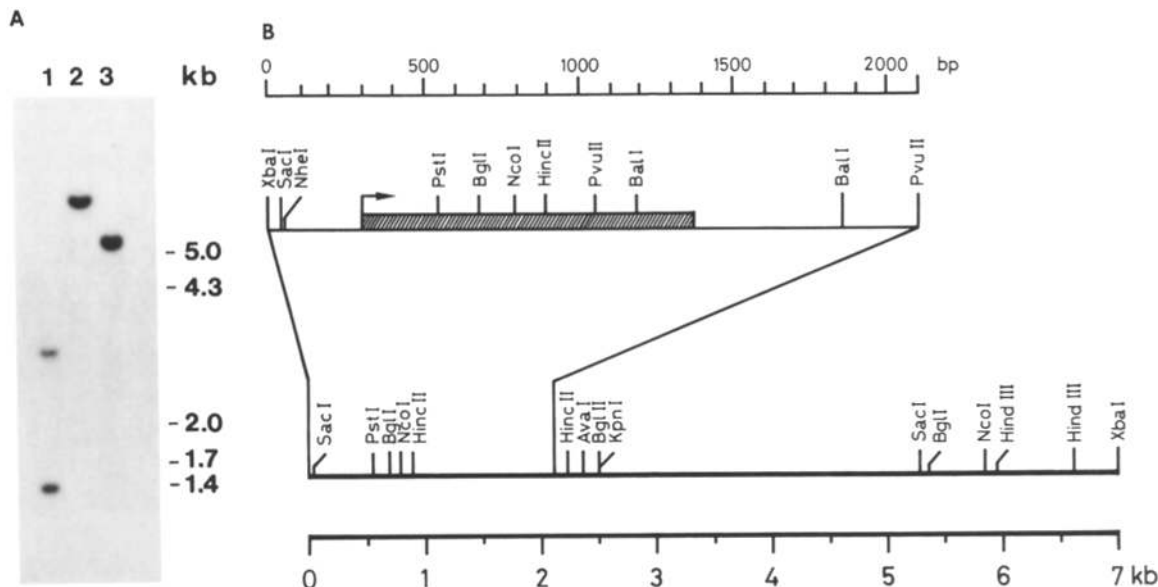


**Figure 2.** (A) Hybridization of mouse Cx40 DNA (PvuII-XbaI fragment) to a Southern blot of mouse genomic DNA digested with HincII (lane 1), XbaI (lane 2), and BamHI (lane 3). The sequence shown in Fig. 1 contains one restriction site (at position 580) for HincII, but no sites for BamHI and XbaI. The number of bands seen in each lane is consistent with the notion that a single copy of the Cx40 gene exists in the haploid genome. (B) Restriction map of the mouse genomic XbaI fragment containing the Cx40 coding region. The XbaI-PvuII fragment used for sequence determination is enlarged. The coding region of Cx40 and its orientation is indicated by a hatched box with arrow at the ATG start codon.

HincII restriction site in the Cx40 coding sequence (see Fig. 1, position 580, and Fig. 2 B). The human gene for Cx40 has recently been assigned together with the gene for human Cx37 to chromosome 1 (Willecke et al., 1990b).

We have also isolated and characterized phage clones that contained the mouse Cx43 coding sequence. This DNA sequence codes for 382 amino acids like the corresponding rat DNA but shows one amino acid exchange at position 341 (region E in Table I), i.e., a serine residue in mouse instead of the asparagine residue in rat Cx43 DNA (99.7% amino acid identity). The nucleotide sequence of the mouse Cx43 coding sequence shows 52 conserved exchanges compared to the rat sequence (95% identity). In addition we have sequenced 150 bp upstream and 625 bp downstream of the mouse Cx43 coding region. We found a possible splice acceptor site in

consensus context at position -10 or -13 and a possible lariat consensus motif at position -41 upstream of the translation start codon, suggesting the end of an intron. We speculate that another intron may begin at position 1500 in the 3' noncoding region of mouse Cx43 based on comparison with the rat heart Cx43 cDNA sequence (Beyer et al., 1987). Rissek et al. (1990) have reported that rat granulosa Cx43 cDNA differs from rat heart Cx43 cDNA in the 3' untranslated region. The mouse Cx43 genomic sequence determined in our laboratory is deposited in the EMBL/GenBank/DDBJ under accession no. X62836. The nucleotide and amino acid sequence of the coding region of mouse Cx43 has recently been published (Beyer and Steinberg, 1991). In contrast to these data which were generated with oligonucleotide primers, derived from rat Cx43, and the polymerase chain

**Table I. Amino Acid Identities of the Putative Topological Domains of Mouse Cx40 Compared with Mouse Cx43, Mouse Cx32, and Chick Cx42**

Putative topological region of mouse Cx40	Residues in Cx40 sequence	Amino acid identities		
		to mouse Cx32	to mouse Cx43	to chick Cx42
		%	%	%
Cytoplasmic region A	1-22	45 (55)	55 (59)	95 (100)
Transmembrane region 1	23-42	65 (90)	80 (95)	95 (95)
Extracellular region B	43-75	64 (76)	73 (85)	76 (82)
Transmembrane region 2	76-95	55 (70)	70 (90)	95 (100)
Cytoplasmic region C	96-147	25 (33)	24 (33)	56 (68)
Transmembrane region 3	148-167	35 (50)	50 (70)	75 (95)
Extracellular region D	168-204	50 (58)	49 (73)	84 (95)
Transmembrane region 4	205-224	45 (70)	40 (70)	85 (95)
Cytoplasmic region E	225-358	12 (14)	28 (36)	50 (53)

The values in brackets indicate nonidentical amino acids of similar properties, for example Lys vs. Arg. The subdivision of the connexin amino acid sequences was carried out by analogy to the established topological models of Cx32 (Milks et al., 1988; Yancey et al., 1989). Numbers refer to transmembrane regions and letters to cytoplasmic and extracellular regions.

reaction, we found three conservative nucleotide exchanges at the beginning and at the end of the Cx43 coding region. These exchanges are at position 9 (C instead of T reported by Beyer and Steinberg, 1991) at position 15 (C instead of T), and at position 1146 (T instead of C) relative to the start codon at position 1. The mouse Cx43 amino acid sequence determined in our laboratory is the same as reported by Beyer and Steinberg (1991) but differs at positions 320 and 341 from the mouse Cx43 sequence recently published by Nishi et al. (1991). Mouse genomic Cx32 DNA codes for the same amino acid sequence as the corresponding rat DNA (Hennemann et al., 1992; cf. Willecke et al., 1990a).

### Comparison of the Cx40 Sequence with Other Connexin Sequences

The predicted amino acid sequence of mouse Cx40 (Fig. 1) has similar features to other connexins, the topology of which have been directly investigated by site-specific antibodies and membrane protection from proteolysis (Cx32, Zimmer et al., 1987; Milks et al., 1988; Goodenough et al., 1988; Hertzberg et al., 1988; Cx43, Yancey et al., 1989; Cx26, Zhang, J. T., and B. J. Nicholson, manuscript submitted for publication). When the Cx40 amino acid sequence was analyzed according to Rao and Argos (1986) for the tendency to form transmembrane regions, four transmembrane regions were obtained as expected from amino acid sequence alignments with other connexins. Each of the two putative extracellular loops of mouse Cx40 contains three cysteine residues of the sequence CX<sub>6</sub>CX<sub>3</sub>C and CX<sub>4</sub>CX<sub>3</sub>C. Table I shows the predicted pattern of amino acid identities between mouse Cx40, mouse Cx43, mouse Cx32 (Hennemann et al., 1992), and chick Cx42 (Beyer et al., 1990) according to topological domains, as established for Cx32 and Cx43 previously (Milks et al., 1988; Hertzberg et al., 1988; Beyer et al., 1989; Yancey et al., 1989). It is evident that mouse Cx40 has greater similarity with chick Cx42 than with any other mouse connexin sequences. In particular the cytoplasmic regions C and E, which show the highest divergence among connexins, exhibit ~50% amino acid identity between mouse Cx40 and chick Cx42, although the chick sequence is seven amino acids longer. The balance of the molecules comprising the amino-terminal domain A, and the putative extracellular and transmembrane domains, exhibit ~85% amino acid identity. Thus we conclude that Cx40 in mouse and Cx42 in chick are likely to be analogues.

The amino acid sequence of mouse Cx40 exhibits several consensus motifs for possible posttranslational modification. For example at position 342–345 the sequence RRXS (also found in the chick Cx42 sequence) could be a substrate for cAMP-dependent protein kinase and the multifunctional calmodulin-dependent protein kinase II. There are several possible sites of phosphorylation by casein kinase I (S/EXXS) and by casein kinase II (SXXE) in the putative cytoplasmic regions of mouse Cx40 (Kemp and Pearson, 1990). A possible *N*-glycosylation site at position 273–275 of mouse Cx40 (NXS/T) is unlikely to be used since current topological models would place it in the cytoplasm.

### Expression of Cx40 mRNA

Fig. 3 illustrates the results obtained after Northern blot hybridization of total RNAs from several tissues to a Cx40 genomic probe (PstI–PvuII fragment of coding region) (top)

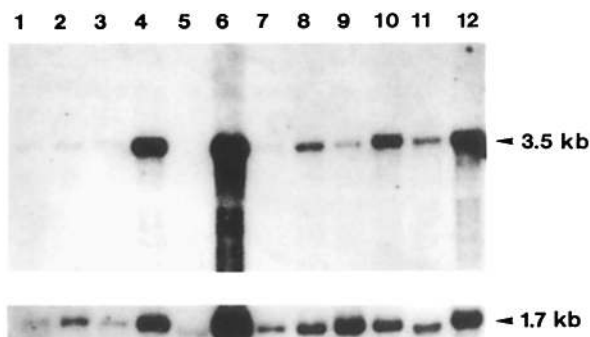


**Figure 3.** (Top) Tissue-specific expression of Cx40 RNA as detected after Northern blot hybridization and autoradiography. 20  $\mu$ g of total mouse RNA from adult tissues: intestine (lane 1), brain (lane 2), skin (lane 3), heart (lane 4), liver (lane 5), lung (lane 6), spleen (lane 7), kidney (lane 8), and embryonic tissues: brain (lane 9), skin (lane 10), liver (lane 11), and kidney (lane 12), were probed at high stringency with the 0.5-kb PstI–PvuII fragment of the Cx40 coding region. Although RNA levels in the lung were at least 16-fold higher than in any other tissue, strong signals were also detected in kidney, skin, and heart, with embryonic levels typically being higher than in the adult. (Bottom) Autoradiograph of Northern blot hybridization using the same RNA blot as above but probing with mouse Cx37 cDNA (Willecke et al., 1991a) (for details see Materials and Methods).

and the Cx37 cDNA (bottom) under stringent conditions of hybridization (42°C, 55% formamide, 5 $\times$  SSC). Single transcripts of 3.5 and 1.7 kb, respectively, were detected in most tissues tested. The same Northern blot was also hybridized to mouse cytochrome c oxidase cDNA (not shown), the resulting autoradiograph was densitometrically evaluated and used as standard for the amount of poly(A)<sup>+</sup> RNA. Cx40 and Cx37 transcripts are more abundant in lung than in any other tissue tested. Overall, the patterns of expression found for each connexin were similar, although the level of Cx40 mRNA was significantly higher in embryonic kidney, skin, and in adult heart, while Cx37 mRNA was more abundant in embryonic brain. However, the message for both is at least 16-fold higher in lung than in any other adult tissue examined. By hybridizing both probes to the same Northern blot of lung RNA and correcting for length and specific activity (results not shown), we determined that the 3.5-kb Cx40 transcript is present at 1.2-fold the level of the 1.7-kb Cx37 transcript. In embryonic kidney, skin, brain, and liver the level of Cx40 transcripts is three- to four-fold higher than in the corresponding adult tissues. Weak expression of mouse Cx40 was also found in the endometrium and myometrium of rat uterus in pregnant and nonpregnant animals (results not shown). While a significant increase in Cx40 mRNA was noticed in endometrium close to term, similar to that found for Cx26 and Cx43 (Winterhager et al., 1991), no change was seen in myometrium.

### Functional Expression of Mouse Cx40 in *Xenopus* Oocytes

To determine if Cx40 is competent to form intercellular channels, and how the properties of such channels compare with those of other connexins, we used the paired *Xenopus* oocyte expression system described in Barrio et al. (1991),

and Willecke et al. (1991b). In this study, all oocytes used had resting potentials of  $45 \pm 10$  mV and were clamped within 5 mV of their resting potential. Background from coupling through endogenous connexins was eliminated by injection of an antisense oligonucleotide to bases 327 to 358 of *Xenopus* Cx38 (Ebihara et al., 1989) (compare the data of H<sub>2</sub>O/H<sub>2</sub>O to anti/anti in Table II). Coinjection with the cRNA to be expressed (i.e., Cx40) served also to greatly reduce coupling with oocytes injected only with H<sub>2</sub>O or antisense oligonucleotides (Cx40/H<sub>2</sub>O and Cx40/anti Table II; compare results in Barrio et al., 1991). In some instances, the exogenous connexin can induce expression of the endogenous protein in the apposed oocyte (e.g., Cx43, Swenson et al., 1989; Werner et al., 1989; Cx37, personal observation). In these cases, injection of antisense oligonucleotide 1 wk before cRNA injection and oocyte pairing was necessary to eliminate endogenous contributions to coupling.

When both oocytes of the pair received Cx40 cRNA along with *Xenopus* Cx38 antisense oligonucleotide, mean levels of conductance were 200–1,000-fold higher than the controls (either anti/anti or Cx40/anti in Table II). The actual induction of coupling was significantly higher, but pairs with junctional conductance ( $G_j$ )  $> 5 \mu\text{S}$  were not used in the analysis. This was necessary to minimize systematic errors in the measurement of the actual transjunctional voltage drop ( $V_j$ ). At higher junctional conductances, access resistance, contributed mainly by the cytoplasm, contributes significantly to the voltage drop between the clamping electrodes in each cell, leading to an overestimation of the actual  $V_j$  and an underestimation of the voltage sensitivity of the junctional channels (Jongsma et al., 1991).

The voltage gating of the Cx40 gap junctions between oocytes shows markedly distinct characteristics from those of other connexins that have been recorded under similar conditions in this system (Fig. 4 and Table III). Junctional current decayed exponentially with time as transjunctional voltage of either polarity was increased across the junction (Fig. 4). The time constant of this decay decreased with  $V_j$  and, while much slower than voltage-gated Na<sup>+</sup> and K<sup>+</sup> channels, was approximately twofold faster than the slow response of Cx37 channels (Willecke et al., 1991 a,b) and 10-fold faster than the responses of Cx26 or Cx32 channels (Barrio et al., 1991) (see Table III).

Initial conductance, measured at the beginning of each

**Table II. Intercellular Conductances of Paired *Xenopus* oocytes**

Injection	Mean junctional conductance ( $G_j$ )	SD	n experiments/ n oocyte pairs
	$\mu\text{S}$		
H <sub>2</sub> O/H <sub>2</sub> O	0.053	0.065	10/24
Anti/anti*	0.0023	0.0016	9/21
Cx40/anti*	0.012	0.007	3/5
Cx40/H <sub>2</sub> O	0.011	0.008	2/4
Cx40/Cx40†	2.5	2.3	8/8
Cx40/Cx37‡	1.6	1.3	5/6

\* "Anti" means antisense oligonucleotide to *Xenopus* Cx38 (327–358). A similar antisense oligonucleotide to *Xenopus* Cx43 had no effect on endogenous coupling.

† All oocytes receiving connexin cRNA were co- or preinjected with antisense oligonucleotide to *Xenopus* Cx38.

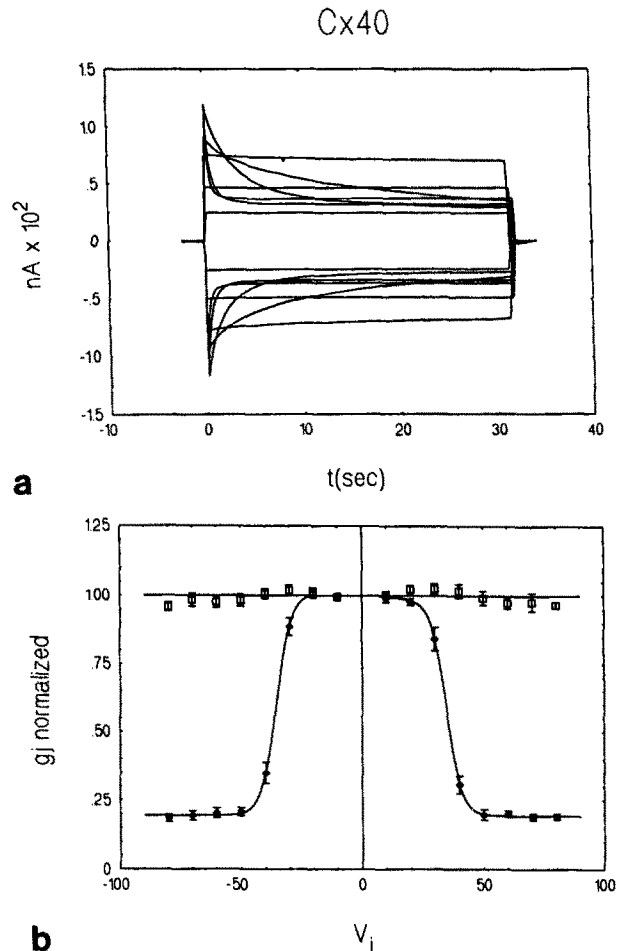


**Figure 4.** Voltage-dependent properties of junctional coupling between paired *Xenopus* oocytes coinjected with mouse Cx40 cRNA and an antisense oligonucleotide to the endogenous *Xenopus* Cx38 (nucleotides 327 to 358). (a) Traces show the decay of junctional current in response to  $\pm 10$ -mV increments in transjunctional voltage ( $V_j$ ) from a resting potential of  $-45$  mV on each oocyte. Each is described by a simple exponential function with decreasing time constant for increasing  $V_j$ . (b) Initial and steady-state values of junctional conductance— $G_j$  (i) (□) and  $G_j$  (ss) (◇), respectively—obtained by extrapolation of the current traces to zero or infinity, respectively, are plotted against  $V_j$ . Each point represents the mean and SD of recordings from eight oocyte pairs. The steady-state data are computer fitted to symmetrical Boltzmann equations, the parameters of which are given in Table III.

30-s voltage step by extrapolation of the exponential current decay to zero time, was ohmic. This observation, in conjunction with the superimposition of currents obtained from oocyte pairs with the same  $V_j$ , but different initial holding potentials ( $-40$ ,  $-20$ , and  $0$  mV—data not shown), demonstrated the absence of any transmembrane ( $V_{j\rightarrow}$ ) sensitivity in this channel. Steady-state conductance showed a steep and symmetrical reduction with increasing  $V_j$  of either polarity to a minimum value of  $\sim 20\%$  of initial levels. The  $V_j$  dependence of steady-state  $G_j$  (normalized to the initial  $G_j$  value at  $\pm 10$  mV) was well fit by the Boltzmann equation described in Spray et al. (1981) and shown in Table III with the following parameters:  $V_0 = \pm 35$  mV;  $A = 0.32$ ;  $G_{\min} = 0.19$  (based on experiments with eight oocyte pairs).

Table III. Boltzmann Parameters of Voltage Gating of Different Connexins Expressed in *Xenopus* Oocytes

Connexin expressed	$V_0^*$	$A^* (n)^\ddagger$	$G(\text{min})^\S$	$T(\text{s})^\parallel$	Reference
	<i>mV</i>				
Mouse Cx40	35	0.32 (8)	0.19	0.58	Present work
Mouse Cx37 - slow <sub>1</sub>	16	0.44 (11)		0.95	Willecke et al., 1991
slow <sub>2</sub>	40	0.09 (2)	0.12	ND	
fast	60	0.09 (2)	0.40	<0.002	
Mouse Cx40/37 hybrids <sup>†</sup>					Present work
Cx40(+) slow	26	0.33 (8)	0.26	ND	
fast	ND	ND	ND	<0.002	
Cx37(+) slow	19	0.26 (6)	0.30	ND	
fast	51	0.07 (2)	0.18	<0.002	
Rat Cx32**	57	0.09 (2)	0.23	5.6	Barrio et al., 1991 Suchyna, T., personal observations
Rat Cx26	89	0.15 (4)	0.1	6.3	Swenson et al., 1989 Werner et al., 1989
Rat Cx43**	—	—	—	—	

— = No voltage sensitivity.

\* Parameters taken from a fit of the experimental points to a Boltzmann equation of the form  $G_j(\text{ss}) = (G_j[\text{max}] - G_j[\text{min}]) / \{1 + \exp(A[V - V_0])\} + G_j[\text{min}]$ .  $V_0$  = Voltage of half-maximal decrease in  $G_j(\text{ss})$ .  $A$  = Cooperativity constant in  $\text{mV}^{-1}$ .

†  $A$  can be modeled as movement of a number of electrical charges ( $n$ ) across the membrane in response to voltage (i.e., gating charge) where  $n = A \frac{kT}{q}$ . ( $k$  = Boltzmann constant;  $T$  = absolute temperature;  $q$  = elementary charge.)

‡  $G(\text{min})$  = limiting minimal conductance of the channel at high  $V_j$ , normalized to conductance of the channel when fully open ( $G[\text{max}]$ ).

§  $T$  = time constant of exponential current decay in response to  $V_j$  measured at  $V_0 + 15$  mV for each channel (note:  $T$  decreases with  $V_j$ ).

¶ Hybrid channels show asymmetric fast ( $G_j[\text{i}]$  records) and slow ( $G_j[\text{ss}]$  records) responses to  $V_j$ . Data are shown for Cx40 injected side relatively positive, and for Cx37 side relatively positive.

\*\* Parameters shown were obtained independently in the Bennett and Nicholson laboratories and contrast to results reported earlier in more highly coupled oocytes by Swenson et al., 1989 and Werner et al., 1989 (see text for discussion). Moreno et al. (1991) reported different parameters for Cx32 voltage gating than given here using several different systems, suggesting that the preparation can influence these properties. Hence, only data from the *Xenopus* oocyte system are included in the table.

\*\* No voltage sensitivity of Cx43 channels is detected in these oocytes.

These characteristics represent a unique "fingerprint" for this connexin compared with other connexins expressed similarly in oocytes (see Table II). One notable feature is the high level of cooperativity shown by this connexin compared with others, including the endogenous *Xenopus* Cx38 which has a similar  $V_0$  to Cx40 but shows a gradual decrease in  $G_j$  with increasing  $V_j$  (cf. plots shown in Werner et al., 1989). The conductance of Cx40 channels undergoes the complete transition from  $G_j(\text{max})$  to  $G_j(\text{min})$  in the span of just 20 mV (Fig. 4). By classical modeling approaches, this would equate to a gating charge of  $\sim 8$ , higher than that of voltage-gated  $\text{Na}^+$  channels. Only the more sensitive of the two slow gates described previously for Cx37 channels (Willecke et al., 1991 *a,b*) has a comparably high cooperativity constant (Table III).

Given the consistent coexpression of Cx37 and Cx40 in a number of tissues, particularly lung, we also tested the potential for these connexins to interact by pairing oocytes — one injected with Cx40 and the other with Cx37. Asymmetric heterotypic channels did form efficiently, with voltage-gated properties similar to, but modified from, those of the parental homotypic channels (Fig. 5).

Defining the Cx37-injected pole as the positive pole, results for positive  $V_j$  were obtained by both depolarization of the Cx37-injected oocyte, and hyperpolarization of the Cx40-injected oocyte. The inverse procedure was applied for negative  $V_j$  values. In all cases  $G_j(\text{ss})$  was normalized with respect to  $G_j(\text{i})$  at the same  $V_j$  in order to isolate the slower gating responses of the channel from the superimposed influence of faster gating phenomena not resolved by the

voltage clamps. Fig. 5 shows the  $V_j$  vs.  $G_j$  plots of the heterotypic channels superimposed on the plots for homotypic Cx37 (*b*) and Cx40 (*c*) channels. At positive  $V_j$ 's (i.e., Cx37-injected oocyte relatively positive), the steady-state response ( $G_j[\text{ss}]$ ) of the heterotypic channels corresponds most closely to the more sensitive component of  $G_j(\text{ss})$  in Cx37 homotypic channels with similar  $V_0$  (19 cf 15 mV) but reduced cooperativity ( $A = 0.26$  cf 0.44). However, while  $G_j(\text{ss})$  dependence on  $V_j$  in the homotypic channels was described by a linear combination of two Boltzmann equations<sup>1</sup> (see Willecke et al., 1991*b*), the hybrid channels were best fit by a single Boltzmann equation, although deviation of the data from the "fitted" curve was evident, particularly at higher  $V_j$ 's. It should be noted that  $G_j(\text{ss})$  values are normalized to  $G_j(\text{i})$  for each value of  $V_j$ . Since these initial values deviate markedly from ohmic behavior at higher  $V_j$ 's, it is possible that systematic errors in determining  $G_j(\text{ss})$  values could mark a second, less sensitive decay in  $G_j(\text{ss})$ , with  $V_j$  analogous to that seen in the homotypic channels. The voltage sensitivity of  $G_j(\text{i})$ , reflecting a rapid gating of the channels unresolved by the voltage clamps, was more ac-

1. The steady-state response of Cx37 homotypic channels was best fit by a Boltzmann equation where the  $g_{\text{min}}$  was itself a Boltzmann function. Looked at another way, the junctional conductance was determined by a linear combination of two Boltzmann decays with  $g_j(\text{min})$  of one equal to  $g_j(\text{max})$  of the second; i.e.,

$$g_j = [g_j(\text{max})_1 - g_j(\text{min})_1] / \{1 + \exp[A_1(V_j - V_{01})]\} + [g_j(\text{max})_2 - g_j(\text{min})_2] / \{1 + \exp[A_2(V_j - V_{02})]\} + g_j(\text{min})_2 \text{ where } g_j(\text{max})_2 = g_j(\text{min})_1.$$

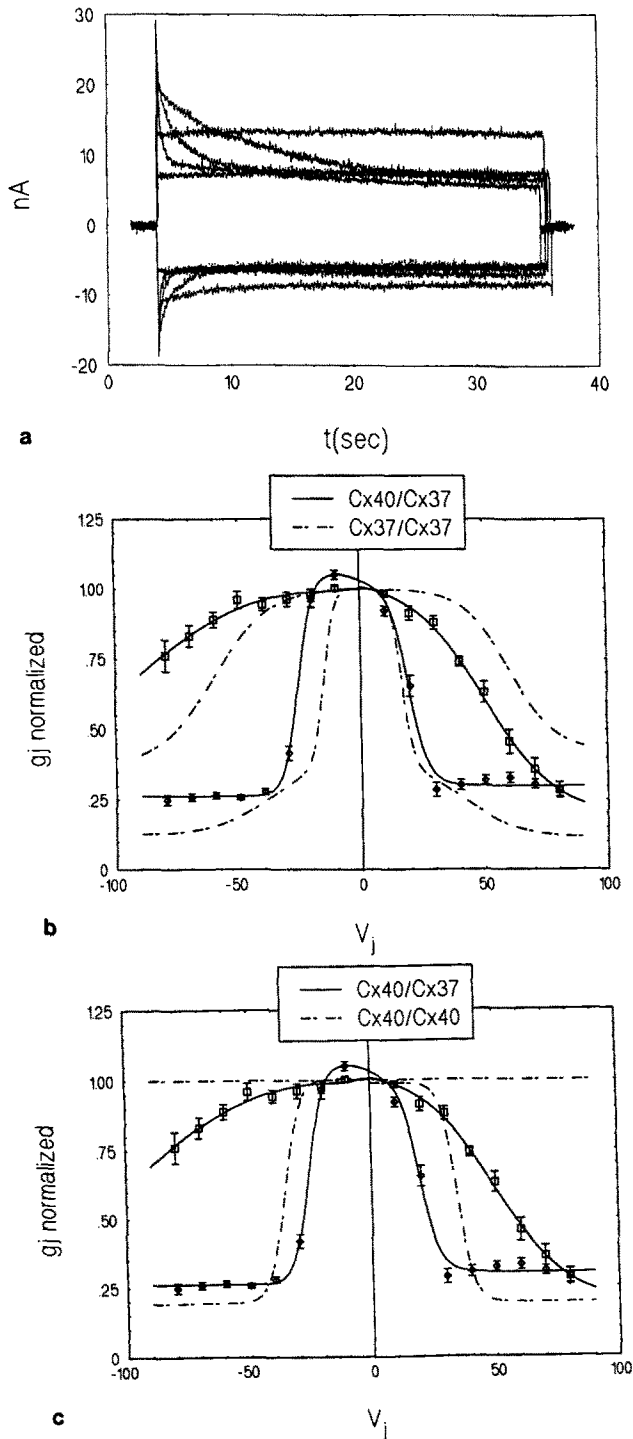


**Figure 5.** Voltage dependencies of junctional coupling between paired *Xenopus* oocytes—one injected with Cx37 cRNA and the other with Cx40 RNA. Both oocytes also received antisense oligonucleotides to *Xenopus* Cx38. The Cx37-injected oocyte is defined as the positive pole and both oocytes are clamped between  $-40$  and  $-50$  mV. (a) Current traces from the Cx37-injected oocyte in response to voltage steps in the Cx40 oocyte of  $\pm 10$  to  $\pm 50$  mV, in 10-mV increments (virtually identical traces are obtained by recording from the Cx40 oocyte and using the Cx37 oocyte). Initial ( $G_j(i)$ ) and steady-state ( $G_j(ss)$ ) conductances were obtained from exponential fits to these traces and extrapolation to 0 and infinite times, respectively. (b and c) Dependence of  $G_j(i)$  ( $\square$ ) and  $G_j(ss)$  ( $\diamond$ ) on transjunctional voltage ( $V_j$ ).  $G_j(i)$  values are normalized to  $G_j(i)$  at a  $V_j$  of +10 mV, and  $G_j(ss)$  values are normalized to  $G_j(ss)$

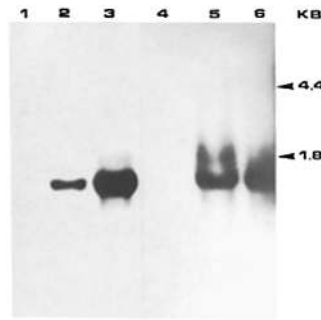


**Figure 6.** Northern blot hybridization of Cx40 transfectants and parental cells. The entire coding region of mouse Cx40 DNA was hybridized under high stringency to electrophoretically separated, total RNA from the following cell lines and autoradiographed: (lane 1) Nontransfected HeLa cells, (lane 2) HeLa transfectant clone D25, (lane 3) HeLa transfectant clone B35, (lane

4) nontransfected SK-Hep-1 cells, (lane 5) SK-Hep-1 transfectant clone E, and (lane 6) SK-Hep-1 transfectant clone B. The transcript size of 1.5 kb is expected for the expression construct pBEHpacl8/Cx40 and is only detected in Cx40 transfectants but not in the parental cells.

centuated in the hybrid channels at positive  $V_j$ 's. Boltzmann fits to the data yielded a lower  $V_o$  (51 cf 60 mV) and  $G_j$  (min) (0.19 cf 0.40) than seen in homotypic Cx37 channels.

At negative  $V_j$  values (i.e., Cx40-injected oocyte relatively positive),  $G_j$  (ss) responses most closely resemble those of the homotypic Cx40 channels. The data were fit well by a single Boltzmann equation with similar  $A$ , but modified  $V_o$  (26 cf 35 mV) and  $G_j$  (min) (0.26 cf 0.19) compared with homotypic Cx40 channels. The hybrid channels also show a small but consistent increase in junctional current with time during small negative steps in  $V_j$ , reflected in the higher mean value for  $G_j$  (ss) compared with  $G_j$  (i) at  $V_j = -10$  mV. A significant deviation of  $G_j$  (i) from ohmic behavior is also detected at negative  $V_j$ 's in the hybrid channels. However, insufficient data are available to define a unique Boltzmann equation to fit the data. Although interpretation of the data for heterotypic channels is complicated by apparent allosteric interactions between the hemichannels, the polarity of the responses deduced here is consistent with those of Bennett et al. (1988); Swenson et al. (1989); Werner et al. (1989), and Barrio et al. (1991), where the hemichannel on the positive side of the voltage gradient was deduced to close.

### Functional Expression of Mouse Cx40 DNA in Transfected Human Cells

To study expression of the cloned mouse Cx40 DNA in mammalian cells, we transfected human HeLa and SK-Hep-1

at the same  $V_j$ . All points are the means and SD of six oocyte pairs (five independent experiments), using both depolarizations and hyperpolarizations of each cell. Solid curves are computer fits of the data (Easy Plot; Spiral Software, Brookline, MA) to Boltzmann equations with parameters shown in Table III. The exception is  $G_j(i)$  at negative  $V_j$ 's where data were insufficient to uniquely define the parameters. Duplicate plots are shown in b and c to allow comparison with the analogous plots of homotypic channels comprised of Cx37 (broken curves in b) and Cx40 (broken curves in c). It is evident that the heterotypic channels have voltage gating properties which are not described by a series combination of homotypic hemichannels. However, the curves at positive  $V_j$  (Cx37-injected oocyte, relatively positive) more closely resemble Cx37 homotypic curves (b), while those at negative  $V_j$  (Cx40-injected oocyte, relatively positive) resemble more those of Cx40 homotypic channels (c).



cells with the coding region of mouse Cx40 under control of the SV-40 early promoter/enhancer. Both cell lines were chosen because they show a very low level of dye transfer when microinjected with Lucifer yellow and no connexin transcript after Northern blot hybridization of total RNA. Out of 18 HeLa and 12 SK-Hep-1 transfectants, two clones each were selected for further study. Fig. 6 shows that these transfectants express Cx40 transcripts of  $\sim 1.5$  kb which is the expected size for the fully processed product of the construct pBEHpac18/Cx40. The parental HeLa cells (lane 1) and SK-Hep-1 cells (lane 4) do not show any Cx40 transcript.

The transfectants and parental cells were investigated for gap junctional intercellular communication by transfer of the microinjected fluorescent dye Lucifer yellow. Injections of this dye into HeLa transfectants, clones B35 and D25, yielded communication frequencies with nearest neighbor cells of 78 and 62%, respectively (cf. Fig. 7). 30 successful injections of each cell line were carried out. Dye injections of SK-Hep-1 transfectants, clones B and E, yielded coupling frequencies of 57 and 75%, respectively. No transfer of Lu-

cifer yellow was observed with the parental HeLa as well as SK-Hep-1 cells and with the corresponding Cx40 construct in antisense orientation (data not shown).

### Discussion

In this paper the genomic sequence and the deduced amino acid sequence of the mouse Cx40 gene is described. Although we have not yet isolated the corresponding Cx40 cDNA, there are several findings in support of our conclusion that we have characterized the functional coding region of a new mouse connexin gene: (a) the coding region of Cx40 hybridizes to a 3.5-kb transcript in several mouse tissues; (b) it can be expressed in *Xenopus oocytes* where it forms gap junction channels exhibiting a voltage dependency not found previously for other connexins in this experimental system; (c) it can be expressed in human HeLa and SK-Hep-1 cells and restores gap junctional intercellular communication in the coupling-deficient parental cells; and (d) it appears to be analogous to chick Cx42. The genomic Cx40 sequence has

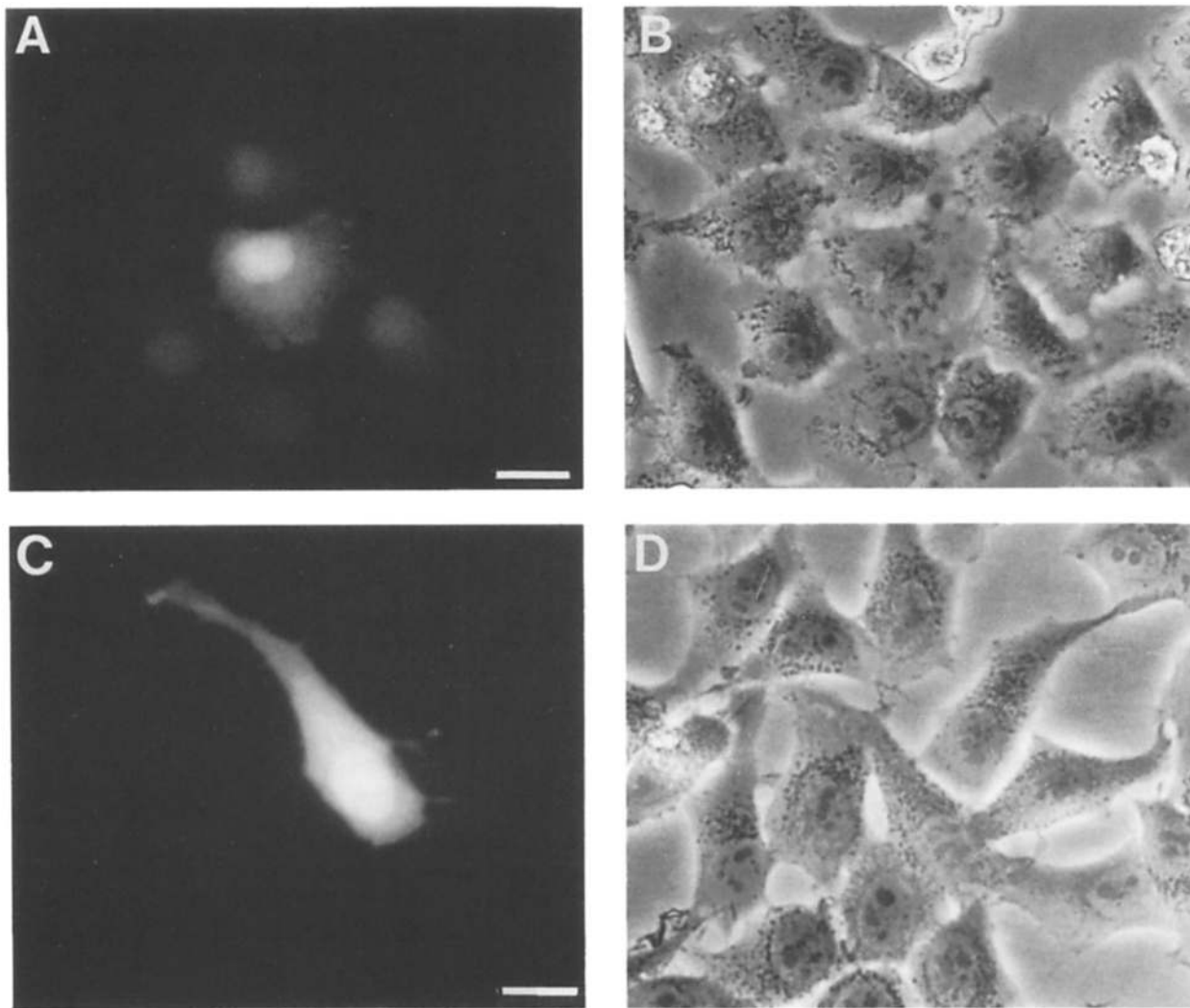


**Figure 7.** Functional expression of mouse Cx40 in transfected human HeLa cells. Cells were microinjected with Lucifer yellow and fluorescence micrographs (A and C) were taken 1 min after microinjection. B and D are phase-contrast micrographs of the same viewfields shown in A and C, respectively. (A and B) HeLa Cx40 transfectant, clone B35; (C and D) nontransfected HeLa cells. Bars, 20  $\mu$ m.

all the features characteristic of other cloned rat or mouse connexin genes, i.e., a reading frame uninterrupted by introns but a possible intron immediately upstream of the initiation site for translation.

Although we have concluded that mouse Cx40 and chick Cx42 are likely to be analogous, based on amino acid identities of ~50% between the highly divergent, putative cytoplasmic domains C and E (see Table I), the overall amino acid identity between both proteins is only ~67%. This is significantly lower than the 93% amino acid identity found between mouse and chick Cx43. This could mean that the function or regulation of Cx40 channels in mouse tissues may be different from that of Cx42 in chick. Alternatively, it is possible that the function of Cx40 is more tolerant of change in the primary sequence than is the case for Cx43. Patterns of tissue expression may give some preliminary indications as to which of these possibilities may apply. Comparisons of Northern blot hybridizations in chick with Cx42 (Beyer et al., 1990) and mouse with Cx40 (this study) indicate that both proteins are expressed in embryonic tissues, adult heart and liver, and embryonic heart (Dahl, E., C. Fromaget, D. Gros, and K. Willecke, unpublished observations). However, it is not known whether chick Cx42 mRNA is as highly abundant in chick lung as are Cx40 transcripts in mouse lung.

Our result that the coding DNA of mouse Cx40, when transfected into coupling-deficient human HeLa or SK-Hep-1 cells, restores gap junctional communication demonstrates the functional integrity of the cloned Cx40 in a homologous cell system. This conclusion is supported by detection of the expected Cx40 transcript in the transfectants. Furthermore, specific expression of the Cx40 protein was found in the transfected but not in parental HeLa or SK-Hep-1 cells based on immunoblot and immunofluorescence analyses using antibodies directed against a COOH-terminal peptide of Cx40 (Traub, O., H. Lichtenberg-Fraté, R. Eckert, D. Hülser, and K. Willecke, manuscript in preparation).

Mouse Cx40 mRNA is 16-fold more abundant in lung than in any other mouse tissue tested, reminiscent of the similar expression pattern for mouse Cx37 (Fig. 3; and Willecke et al., 1991b). While the coexpression of these two proteins may be analogous to that noted for Cx32 and Cx26 (Zhang and Nicholson, 1989), it is currently unknown if they are expressed by the same cells. However, if this analogy is pursued, it is of interest that a consensus motif for *in vivo* phosphorylation by cAMP-dependent kinase is only detected in the COOH-terminal region of Cx40 but not of Cx37, which could lead to differential regulation of the proteins (cf. Traub et al., 1989). Cx40 and Cx37 channels also differ in their voltage gating characteristics, although both channels possess more sensitive (cf.  $V_o$ 's in Table III) and faster gating (cf.  $T_s$  in Table III) than the Cx32 and Cx26 channels. In addition, hybrid channels can form between these connexins, when expressed in apposed oocytes. As proved to be the case with hybrid Cx32/26 channels (Barrio et al., 1991), hybrid Cx40/37 channels have modified properties from the homotypic forms, although to a lesser extent than reported in the previous case. This represents the second documented case of allosteric interactions between hemichannels comprised of different connexins which causes a significant modulation of the intercellular channel properties, at least with respect to their voltage gating.

One notable feature of the gating of both Cx40 and Cx37 homotypic and heterotypic channels is the highly cooperative nature of their closure in response to  $V_j$ . Complete gating of the channels occurs over a range of only 20 mV, corresponding to a Boltzmann cooperativity constant ( $A$ ) of 0.3–0.44 (see Table III). In the classical theory of voltage-gated channels, this is modeled as an equivalent movement of charges (gating charges) across the membrane in response to the imposed voltage gradient. While this approach yielded a gating charge of ~2 for voltage gating of most connexins, it predicts for Cx40 a net movement of 7.5 charges across the channel (and ~11 in the case of the slow response of homotypic Cx37 channels). This could be achieved by partial movement of a larger number of charges the number and/or distribution of which may differ between connexins. However, it is difficult to account for an appropriate distribution of so many charges in the current models of the gap junction. Even in the case of voltage-gated  $\text{Na}^+$  and  $\text{K}^+$  channels, which have an "ideal" arrangement of charges spanning the membrane in their S4 helix, the equivalent gating charge movement only ranges from four to six (Hille, 1984). However, it is possible that the parameter  $A$  in the Boltzmann relation may not only represent the contribution of gating charge to the energy needed for the channel to close, but may also include energy transferred from one closing channel to other open channels in the vicinity, thereby decreasing their activation energy for closure. The close packed nature of connexins in a gap junction makes them ideal candidates for such cooperative interactions, in the same way hemoglobin benefits from neighboring interactions not available to myoglobin. The net effect would be that the gating charge calculated directly from  $A$  by traditional Boltzmann approaches may in the case of gap junctions be a significant overestimation, as it may include a significant contribution from cooperativity between channels which could vary between connexins.

The physiological analysis of Cx40 homotypic and Cx40/37 heterotypic gap junctional channels, presented here, focuses on their gating in response to voltage, although it is possible that this is indicative of differences in other gating responses (e.g., pH,  $\text{Ca}^{++}$ , etc.). It is likely that these responses may not be determined solely by the primary sequence of connexins alone, but could be modified by the cytoplasmic environment in a given cell. Thus, while Cx40 can be expressed functionally in both oocytes as well as mammalian cells (Fig. 7), it is as yet unclear whether the channel properties are identical. However, an advantage of the oocyte system is that it provides a constant environment in which to compare the channel properties of different connexins (Table III). While cytoplasmic factors may modulate gap junction channel function, all connexins expressed in oocytes are exposed to the same factors. Thus differences in their properties must be attributable to the connexin structures themselves. Even in such a constant system, caution must be exercised to maintain comparable conditions. For example, as described in Results, measurement of transjunctional voltage gating can be affected when  $G_j$  between oocytes is too high (Jongsma et al., 1991; Moreno et al., 1991). This leads to an overestimation of actual  $V_j$ , and an underestimation of the voltage sensitivity of the channel. This may explain earlier discrepancies in the reported voltage sensitivity of Cx32 channels in oocytes (cf. Swenson et al., 1989 and Werner et

al., 1989 with Barrio et al., 1991), where the former authors report no sensitivity to  $V_j$  under conditions of very high junctional conductance, unless this is secondarily reduced by pH.

A thorough comparison of different connexins, expressed in the same system under comparable conditions, including analysis of their gating properties and permeabilities to metabolites, will ultimately help to define why there is a need for at least 10 different connexin genes expressed in mouse or rat tissues (Willecke et al., 1991a). Out of these 10 genes, only Cx40 and Cx37 transcripts were found to be much more abundant in lung than in any other tissue. The clarification of the properties of these connexins and their dependence on the primary structure of the proteins is a major task in understanding intercellular communication in the lung.

The expert technical assistance of Ms. Gaby Hallas and Ms. Feng Gao is gratefully acknowledged. We thank Ms. Rita Lange and Dr. Wolfgang Wille (Institut für Genetik, Universität Köln) for the mouse genomic library. Special thanks go to Dr. Charles Fournier (SUNY at Buffalo) for his invaluable insights into the nature of channel gating.

This work was supported by grants from the Deutsche Forschungsgemeinschaft (Wi 270-14/1); SFB 1387 (project C1); Fonds der Chemischen Industrie to K. Willecke; and by grants from the National Institutes of Health (CA 48049 and HL 37109 [subcontract]) and a Pew Scholar award to B. J. Nicholson. The collaboration between the two laboratories in Bonn and Buffalo was further financed by NATO traveling stipends.

Received for publication 8 August 1991 and in revised form 28 February 1992.

## References

- Barrio, L. C., T. Suchyna, T. Bargiello, L. X. Xu, R. Roginsky, M. V. L. Bennett, and B. J. Nicholson. 1991. Voltage dependence of homo- and hetero-typic Cx26 and Cx32 gap junctions expressed in *Xenopus* oocytes. *Proc. Natl. Acad. Sci. USA*. 88:8410-8414.
- Bennett, M. V. L., V. Verselis, R. L. White, and D. C. Spray. 1988. Gap junctional conductance: gating. In *Gap Junctions*. E. L. Hertzberg, and R. G. Johnson, editors. Alan R. Liss, Inc., New York. 287-304.
- Beyer, E. C., and T. H. Steinberg. 1991. Evidence that the gap junction protein connexin43 is the ATP induced pore of mouse macrophages. *J. Biol. Chem.* 266:7971-7974.
- Beyer, E. C., D. L. Paul, and D. A. Goodenough. 1987. Connexin43: a protein from rat heart homologous to a gap junction protein from liver. *J. Cell Biol.* 105:2621-2629.
- Beyer, E. C., D. A. Goodenough, and D. L. Paul. 1988. The connexins, a family of related gap junction proteins. In *Gap Junctions*. E. L. Hertzberg and R. G. Johnson, editors. Alan R. Liss, Inc., New York. 165-175.
- Beyer, E. C., J. Kistler, D. L. Paul, and D. A. Goodenough. 1989. Antisera directed against connexin43 peptides react with a 43-kD protein localized to gap junctions in myometrium and other tissues. *J. Cell Biol.* 108:595-605.
- Beyer, E. C., D. L. Paul, and D. A. Goodenough. 1990. Connexin family of gap junction proteins. *J. Membr. Biol.* 116:187-194.
- Burt, J. M., and D. C. Spray. 1988. Single channel events and gating behaviour of the cardiac gap junction channel. *Proc. Natl. Acad. Sci. USA*. 85:3431-3434.
- Chen, C., and H. Okayama. 1987. High-efficiency transformation of mammalian cells by plasmid DNA. *Mol. Cell. Biol.* 7:2745-2752.
- Chirghrin, J. M., A. E. Przybala, R. Y. MacDonald, and W. J. Rütter. 1979. Isolation of biologically active ribonucleic acid from sources enriched in ribonuclease. *Biochemistry*. 18:5294-5299.
- Ebihara, L., E. C. Beyer, K. I. Swenson, D. L. Paul, and D. A. Goodenough. 1989. Cloning and expression of a *Xenopus* embryonic gap junction protein. *Science (Wash. DC)*. 243:1194-1195.
- Eghbali, B., J. A. Kessler, and D. C. Spray. 1990. Expression of gap junction channels in communication incompetent cells after stable transfection with cDNA encoding connexin32. *Proc. Natl. Acad. Sci. USA*. 87:1328-1331.
- Fishman, G. I., D. C. Spray, and L. A. Leinwand. 1990. Molecular characterization and functional expression of the human cardiac gap junction channel. *J. Cell Biol.* 111:589-597.
- Goodenough, D. A., D. L. Paul, and J. Jesaitis. 1988. Topological distribution of two connexin32 antigenic sites in intact and split rodent liver gap junctions. *J. Cell Biol.* 107:1817-1824.
- Hennemann, H., G. Kozjek, E. Dahl, B. J. Nicholson, and K. Willecke. 1992.

- Molecular cloning of mouse connexins 26 and -32: similar genomic organization but distinct promoter sequences of two gap junction genes. *Eur. J. Cell Biol.* In press.
- Hergert, T., M. Burba, M. Schmoll, K. Zimmermann, and A. Starzinsky-Powitz. 1989. Regulated expression of nuclear protein(s) in myogenic cells that binds to a conserved 3' untranslated region in pro  $\alpha 1$  (I) collagen cDNA. *Mol. Cell. Biol.* 9:2828-2836.
- Hertzberg, E. L., R. M. Disher, A. A. Tiller, Y. Zhou, and R. G. Cook. 1988. Topology of the Mr 27,000 liver gap junction protein. *J. Biol. Chem.* 263:19105-19111.
- Heynkes, R., G. Kozjek, O. Traub, and K. Willecke. 1986. Identification of a rat liver cDNA and mRNA coding for the 28 kDa gap junction protein. *FEBS (Fed. Eur. Biochem. Soc.) Lett.* 205:56-60.
- Hille, B. 1984. *Ionic Channels of Excitable Membranes*. Sinauer Associates, Inc., Sunderland, MA. 383 pp.
- Hoh, J. H., S. A. John, and J.-P. Revel. 1991. Molecular cloning and characterization of a new member of the gap junction gene family, Connexin-31. *J. Biol. Chem.* 266:6524-6531.
- Horst, M., N. Harth, and A. Hasilik. 1991. Biosynthesis of glycosylated human lysozyme mutants. *J. Biol. Chem.* 266:13914-13919.
- Jongsma, H. J., R. Welders, A. C. G. van Ginnothan, and M. E. Rook. 1991. In *Biophysics of Gap Junction Channels*. C. Peracchia, editor. CRC Press Inc., Boca Raton, FL. 162-172.
- Kemp, B. E., and R. B. Pearson. 1990. Protein kinase recognition sequence motifs. *Trends Biochem. Sci.* 15:342-346.
- Krieg, P. A., and D. A. Melton. 1984. Functional messenger RNAs are produced by SP6 in vivo transcription of cloned cDNA. *Nucleic Acids Res.* 12:7057-7070.
- Kumar, N., and N. B. Gilula. 1986. Cloning and characterization of human and rat liver cDNAs coding for a gap junction protein. *J. Cell Biol.* 103:767-776.
- Milks, L. C., N. M. Kumar, R. Houghton, N. Unwin, and N. B. Gilula. 1988. Topology of the 32-kD liver gap junction protein determined by site-directed antibody localizations. *EMBO (Eur. Mol. Biol. Organ.) J.* 7:2967-2975.
- Miller, T., G. Dahl, and R. Werner. 1988. Structure of a gap junction gene: connexin32. *Biosci. Rep.* 8:455-464.
- Moreno, A. P., A. C. Campos de Carvalho, V. Verselis, B. Eghbali, and D. C. Spray. 1991. Voltage dependent gap junction channels formed by connexin32, the major gap junction protein of liver. *Biophys. J.* 59:920-925.
- Nicholson, B. J., R. Dermietzel, D. Teplow, O. Traub, K. Willecke, and J.-P. Revel. 1987. Two homologous protein components of hepatic gap junctions. *Nature (Lond.)*. 329:732-734.
- Nishi, M., N. M. Kumar, and N. B. Gilula. 1991. Developmental regulation of gap junction gene expression during mouse embryonic development. *Dev. Biol.* 146:117-130.
- Paul, D. 1986. Molecular cloning of cDNA for rat liver gap junction proteins. *J. Cell Biol.* 103:123-134.
- Rao, J. K. M., and P. Argos. 1986. A conformational preference parameter to predict helices in integral membrane proteins. *Biochim. Biophys. Acta.* 869:197-214.
- Risek, B., S. Guthrie, N. Kumar, and N. B. Gilula. 1990. Modulation of gap junction transcripts and protein expression during pregnancy in the rat. *J. Cell Biol.* 110:269-282.
- Saez, J. C., D. C. Spray, A. C. Nairn, E. Hertzberg, P. Greengard, and M. V. I. Bennett. 1986. cAMP increases junctional conductance and stimulates phosphorylation of the 27 kDa principal gap junction proteins. *Proc. Natl. Acad. Sci. USA*. 83:2473-2477.
- Sambrook, J., E. F. Fritsch, and T. Maniatis. 1989. *Molecular Cloning: A Laboratory Manual*. Cold Spring Harbor Laboratory, Cold Spring Harbor, NY. 545 pp.
- Spray, D. C., A. L. Harris, and M. V. L. Bennett. 1981. Equilibrium properties of voltage dependent junctional conductance. *J. Gen. Physiol.* 77:77-93.
- Spray, D. C., J. C. Saez, D. Brosius, M. V. L. Bennett, and E. L. Hertzberg. 1986. Isolated liver gap junctions: gating of transjunctional currents is similar to that in intact pairs of rat hepatocytes. *Proc. Natl. Acad. Sci. USA*. 83:5494-5497.
- Swenson, K. I., H. Piwnica-Worms, H. McNamee, and D. L. Paul. 1990. Tyrosine phosphorylation of the gap junction protein connexin43 is required for the pp60<sup>src</sup>-induced inhibition of communication. *Cell Regulation*. 1:989-1002.
- Tabor, S., and C. C. Richardson. 1987. DNA sequence analysis with a modified bacteriophage T7 DNA polymerase. *Proc. Natl. Acad. Sci. USA*. 84:4767-4771.
- Traub, O., J. Look, R. Dermietzel, F. Brümmer, D. Hülser, and K. Willecke. 1989. Comparative characterization of the 21-kD and 26-kD gap junction proteins in murine liver and cultured hepatocytes. *J. Cell Biol.* 108:1039-1051.
- Veenstra, R. D., and R. L. DeHaan. 1986. Measurement of single channel currents from cardiac gap junctions. *Science (Wash. DC)*. 233:972-974.
- Werner, R., E. Levine, C. Rabadam-Diehl, and G. Dahl. 1989. Formation of hybrid cell-cell channels. *Proc. Natl. Acad. Sci. USA*. 86:5380-5384.
- Willecke, K., H. Hennemann, K. Herbers, R. Heynkes, G. Kozjek, J. Look, R. Stutenkemper, O. Traub, E. Winterhager, and B. J. Nicholson. 1990a. Molecular heterogeneity of gap junctions in different mammalian tissues. In *Parallels in Cell-to-Cell Junctions in Plants and Animals*. A. W. Robards, W. J. Lucas, J. D. Pitts, H. J. Jongsma, and D. C. Spray, editors. NATO

- ASI Series, Springer-Verlag, Berlin, London. 21-34.
- Willecke, K., S. Jungbluth, E. Dahl, H. Hennemann, R. Heynkes, and K.-H. Grzeschik. 1990b. Six genes of the human connexin gene family coding for gap junctional proteins are assigned to four different human chromosomes. *Eur. J. Cell Biol.* 53:275-280.
- Willecke, K., H. Hennemann, E. Dahl, S. Jungbluth, and R. Heynkes. 1991a. The diversity of connexin genes encoding gap junctional proteins. *Eur. J. Cell Biol.* 56:1-7.
- Willecke, K., R. Heynkes, E. Dahl, S. Stutenkemper, H. Hennemann, S. Jungbluth, T. Suchyna, and B. N. Nicholson. 1991b. Mouse connexin37: cloning and functional expression of a gap junction gene highly expressed in lung. *J. Cell Biol.* 114:1049-1057.
- Winterhager, E., R. Strominger, O. Traub, E. Beyer, and K. Willecke. 1991. Expression of different connexin genes in rat uterus during decidualization and at term. *Eur. J. Cell Biol.* 55:133-142.
- Yancey, S. B., S. A. John, L. Ratneshwar, B. J. Austin, and J.-P. Revel. 1989. The 43-kD polypeptide of heart gap junctions: immunolocalization, topology, and functional domains. *J. Cell Biol.* 108:2241-2254.
- Zhang, J. T., and B. J. Nicholson. 1989. Sequence and tissue distribution of a second protein of hepatic gap junctions, cx26, as deduced from its cDNA. *J. Cell Biol.* 109:3391-3401.
- Zimmer, D. B., C. R. Green, W. H. Evans, and N. B. Gilula. 1987. Topological analysis of the major protein in isolated rat liver gap junctions and gap junction-derived single membrane structures. *J. Biol. Chem.* 262:7751-7763.